JOURNAL OF MATERIALS SCIENCE 18 (1983) 2785–2797

# Kinetics of shear-activated indentation crack initiation in soda-lime glass

B. R. LAWN, T. P. DABBS*, CAROLYN J. FAIRBANKS
*Center for Materials Science, National Bureau of Standards, Washington, DC 20234, USA*

The initiation of radial cracks in Vickers indentation of soda-lime glass is found to be strongly rate dependent. For long contact durations the radial cracks pop in during the indentation event, at a reproducible stage of the unloading half-cycle; for short contacts the pop-in occurs after the event, with considerable scatter in delay time. The phenomenon is interpreted in terms of an incubation time to develop a critical nucleus for the ensuing fracture. Increasing either the water content of the environment or the peak contact load diminishes the incubation time. Scanning electron microscopy of the indentation patterns indicates that the sources of the crack nuclei are constrained shear faults within the deformation zone. A qualitative model is developed in terms of a two-step process, precursor faulting followed by crack growth to pop-in instability. Moisture may influence both these steps, in the first by interfacial decohesion and in the second by slow crack growth. No definitive conclusion is reached as to which of the steps is rate-controlling, although it appears that it is the shear across the fault and not the tension across the crack which is vital in driving the initiation. The implications of these results in connection with the basic mechanical properties of brittle solids, particularly strength, are considered.

## 1. Introduction

The strength of brittle materials is controlled by the presence of small flaws [1]. It is generally asserted that such flaws are inevitable and ubiquitous, and that they have the characteristics of true microcracks. Structural design with glasses and ceramics has accordingly centred around the laws of crack *propagation*, the province of "fracture mechanics". However, there is growing evidence that below a threshold size the severity of flaws undergoes an abrupt decrease with an attendant shift in focus to the mechanics of crack *initiation* [2–6]. Whether the sub-threshold flaws retain the essential character of microcracks (albeit within the stabilizing confines of a localized nucleation field) or whether some alternative precursor stress-concentrating process is involved is an issue which remains largely unanswered† [7]. Naturally occurring flaw centres are, by virtue of their small scale (typically $\approx \mu$m), difficult to locate and observe during their evolution to full-scale fracture.

It is in this context that indentation techniques are particularly useful [8]. Flaws can then be generated artificially, with complete control of shape, size and site. Moreover, such flaws bear a strong resemblance to those which develop in structural components from general surface handling, machining and polishing, and in-service particle impact. Insofar as crack initiation from indentation flaws is concerned there has been some revealing, if limited, progress in the development of a fundamental understanding. A theoretical model of crack "pop-in", based on the instability requirements of a critical nucleus within a highly inhomogeneous elastic/plastic contact

*On leave from University of New South Wales, Australia.
†Or, perhaps more accurately, unquestioned, particularly by those who use fracture-mechanics-based theories to analyse the strength properties of optical fibres.

0022–2461/83 $03.00 + .12 © *1983 Chapman and Hall Ltd.*

field, was first presented by Lawn and Evans [2]. However, that model was somewhat phenomenological in that it made no attempt to specify the source of the nucleus, assuming only that such sources were freely available. Subsequent studies of the indentation fracture event identified the key role of irreversible processes in the contact field as a generator of the driving force for pop-in [9, 10], consistent with the general observation that much of the crack formation occurs during unloading of the indenter. A closer investigation of precursor initiation micromechanisms was made in silicate glasses by Hagan and Swain and co-workers [11–14], building on some earlier observations by Peter [15]. This work showed that the contact deformation zone beneath a Vickers or Knoop indenter consisted of well-defined, closely spaced shear faults, at least in glasses with a high content of network modifier, and that the cracks emanated either directly from the faults themselves or from points of intersection with neighbours [14]. The nature of the shear fault interface in terms of its structural properties remains obscure, although the fact that intrinsically strong glass test pieces can be made to fail from sub-threshold indentation flaws at well below theoretical strength indicates that some of the original interfacial cohesion must have been lost [4, 16].

One aspect of indentation crack initiation which has received little attention to data is rate dependence. Rate effects have been shown to be extremely strong in general fracture and deformation properties of several brittle systems, most notablyin silicate materials (both amorphous and crystalline) in the presence of water [17–22]. One of the most dramatic illustrations of a kinetic component in the crack initiation is to be found in the "dynamic fatigue" response of glass test pieces with sub-threshold flaws; the strengths in moist environments drop off more rapidly with decreasing stressing rate than for the corresponding flaws *with* well-developed cracks, notwithstanding the fact that these sub-threshold strengths are greater in magnitude (typically by a factor 2 to 4 [4, 16]) and are subject to much larger scatter [16]. Thus, quite apart from their bearing on the fundamental micromechanics of fracture initiation, rate processes would appear to be of some importance in determining the limits of practical strength, e.g. with optical fibres.

In this paper we investigate the kinetics of "radial" crack [8] initiation in Vickers-indented soda-lime glass in the presence of moist environments as a function of contact time. This is done with an experimental arrangement which allows for *in situ* observation of the contact from below and for control of the load–time characteristics. Post-indentation examination in the scanning electron microscope (SEM) is used to investigate fine details in the deformation and fracture patterns. It is concluded that the initiation event, although driven to its ultimate well-developed configuration by the tensile component of the indentation stress field, is controlled in its kinetics by a precursor, shear-activated process. This process appears to be one of stress intensification, either by interfacial decohesion or by conventional subcritical microcrack growth.

## 2. Observation of crack pop-in kinetics

### 2.1. Experimental procedure

Fig. 1. shows the experimental set-up, a somehwat simplified version of earlier indentation arrangements [9, 23], used in this study. As-received soda-lime microscope slides were loaded from above using a standard Vickers hardness indenter. The indenter arm was driven by an electromagnetic coil via a function generator, and the corresponding load–time pulse $P(t)$ monitored by a piezoelectric transducer [24]. In our tests the pulse had the form of a half-sine wave of height $P_m$ and base width $T$, Fig. 2. A microscope facility enabled an observer to follow the contact event from below the glass slide at all times during and after the loading cycle.

By this means it was observed that the characteristic radial crack pop-in process was highly rate dependent. In particular, the time, $t_c$, to

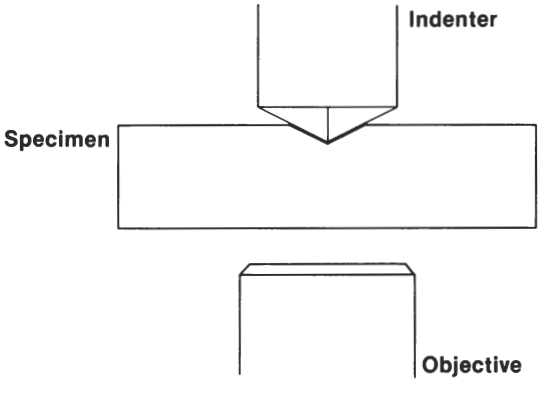


*Figure 1* Schematic of set-up for viewing Vickers indentation in soda-lime glass.

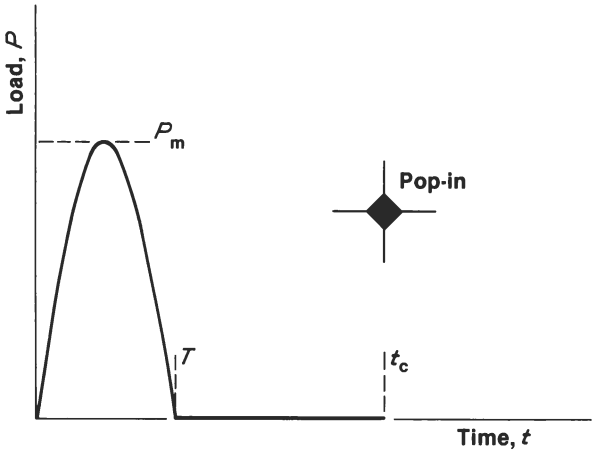


*Figure 2* Indentation load pulse parameters. Experiment measures time to radial crack pop-in, $t_c$, as a function of contact period, $T$, at fixed peak load, $P_m$.

radial crack initiation was sensitive to the contact duration, $T$, for a fixed peak load and environment [25]; whereas for sufficiently large $T$ pop-in occurred during the contact (specifically, during the unloading half-cycle), at small $T$ it showed a tendency to prolonged post-contact delay. The radial crack pattern itself showed some variation from the ideal geometry depicted in Fig. 2; the four arms did not always pop-in simultaneously (in which case $t_c$ was measured on the appearance of the first arm), and nor did they always appear to emerge exactly from the indentation corners. The appearance of each arm was invariably abrupt, without any apparent precursor growth stage.

Test runs were made to determine the dependence $t_c(T)$, and the influence on this dependence of peak contact load and environmental moisture content. The latter test variable was controlled by simple means: laboratory air of relative humidity $50 \pm 5\%$ was taken as a standard environment; extremes of moisture were obtained on the one hand by placing a drop of distilled water on to the prospective indentation site and on the other by enclosing the entire indentation system within a nitrogen gas chamber (although no attempt was made here to ensure optimum "dryness"). The laboratory temperature for these runs was $22 \pm 2^\circ$ C. Some miscellaneous tests were also run to examine the potential effects of extraneous variables, such as surface stress in the glass and post-indentation heating, on delayed pop-in kinetics.

## 2.2. Results

The main results of the kinetic pop-in study are summarized in Figs. 3 to 5. Fig. 3 shows results in detail for a typical test run, in this case in air at load $P_m = 0.7$ N. An average of 15 indentations was made at each of the preselected contact periods $T$. The plot indicates median values as well as individual points in order that the data trends be more clearly distinguishable where the scatter is high. It is immediately apparent that the initiation response differs significantly at opposite extremes of the contact time axis:

(i) At long times pop-in occurred reproducibly *during* the contact at an unload time $t_c \simeq 0.9\,T$.

(ii) At short contact times pop-in occurred *after* indenter release at irregular, extended delay times $t_c \gg T$.

The results shown in Fig. 3 suggest the existence of an incubation time for the development of a

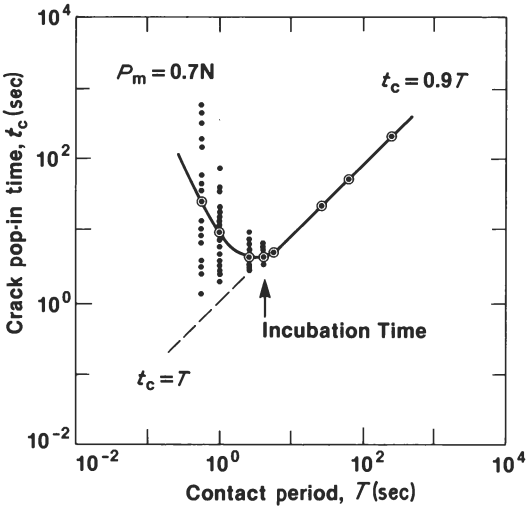


*Figure 3* Time to fracture as a function of contact period, for soda-lime glass in air at fixed indentation load. Open symbols denote median values at each prescribed contact period. Data suggest an incubation time for development of a critical crack nucleus.

critical precursor crack nucleus. This incubation time may be defined (somewhat arbitrarily) as the point where the empirically fitted data curve crosses the line $t_c = T$. For contacts shorter than the incubation time the evolution toward a critical nucleus clearly continues after loading, but at a much reduced rate; that is, the component of the indentation stress which drives the nucleation persists in the residual field, but at a significantly lower intensity than at the peak load configuration. The nucleation event has a stochastical element, as is evident from the scatter in results at small $T$; at large $T$ attainment of a critical condition is guaranteed, and pop-in occurs spontaneously during indenter withdrawl due to release of some stress constraint.

Fig. 4a shows the effect of different peak loads on the kinetics, again in air environment. Over the range of values covered, about one order of magnitude, the load influence does not appear to be strong. Effectively, the results in Fig. 4a may be represented, within the limits of data scatter, by some simple inverse relation between peak load and incubation time. Thus at small $T$ an increased load gives rise to a corresponding reduced (average) pop-in delay. At large $T$ the in-cycle pop-in time does not depend on load. This latter point is illustrated more clearly in the data replot of Fig. 4b, in which the time to fracture is normalized and expanded on to a more sensitive scale. The apparent existence of a load-invariant critical indentation configuration for well-developed nuclei at $t_c = (0.90 \pm 0.05)\ T$, corresponding to $P_c = (0.30 \pm 0.05)P_m$ on the unload half-cycle, indicates that radial crack propagation is controlled by some characteristic of the stress field, independent of the preceding kinetic formation processes.

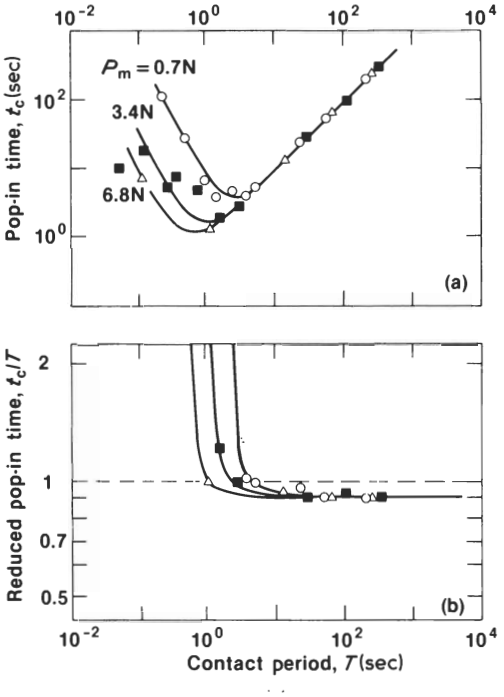


*Figure 4* Time to fracture as a function of contact period, for soda-lime glass in air at three indentation loads. Only median values of pop-in times are plotted. Plot (b) is a replotted version of (a), demonstrating more sensitively the tendency to an equilibrium pop-in condition at longer contact periods.

The influence of environment is shown in Fig. 5, for a given load. It is immediately clear that the incubation time is highly sensitive to moisture content. Thus whereas the introduction of water has no measurable effect on the response at high $T$, consistent with the conclusions drawn from the results in Fig. 4, the pop-in time at low $T$ is dramatically reduced.

The following simple tests were also run in an attempt to gain further clues as to the initiation mechanics:

(i) Some indentations which produced well-developed radial crack patterns on unloading were subjected to repeat loading pulses. On reloading, the radial cracks were observed to close up somewhat at the surface, and conversely to open up further beneath the surface (as observed

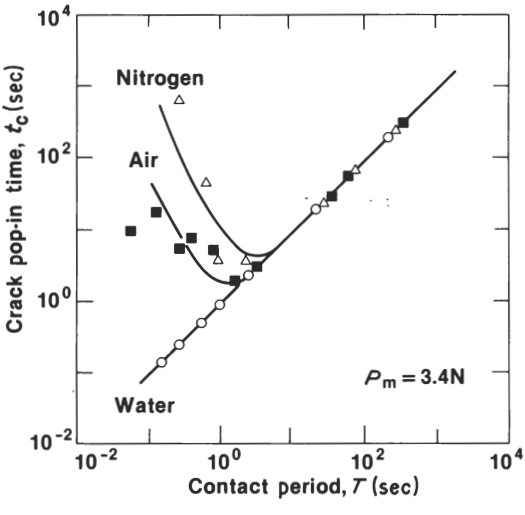


*Figure 5* Time to fracture as function of contact period, for soda-lime glass at fixed indentation load in three environments. Only median values of pop-in times are plotted.

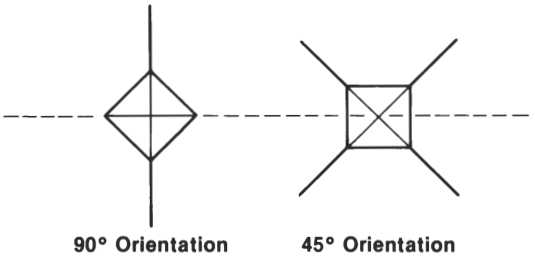


*Figure 6* Schematic of two indentation orientations at pre-existing crack (dashed line) for obtaining section views.

by refocusing the microscope objective, Fig. 1). On reloading beyond the preceding critical unload point $P_c$ the surface closure appeared to be effectively complete, indicating a highly compressive stress in this region.

(ii) Some tests were made on thermally tempered surfaces of a glass of similar composition to that used in obtaining the data for Figs. 3 to 5. Indentations at air at $P_m = 0.7$ N, cf. Fig. 3, produced no radial cracks at all within several hours of unloading. This demonstrates that biaxial surface compressions inhibit the initiation process.

(iii) A row of indentations was produced in air at $P_m = 0.15$ N such that, after an interval of several minutes, the fraction of radial cracks popped in remained small ($\ll 0.5$). After immersing the freshly indented specimen into water at 50° C for about one minute, crack patterns were observed to have developed at all indentations.

## 3. Scanning electron microscopy

### 3.1. Survey of the technique

Although perfectly adequate for determining the critical pop-in points for radial fracture, optical microscopy proved limited as a means of observing fine details in the precursor deformation process. Scanning electron microscopy (SEM) was accordingly used to examine indentation sites after the event. The observations were of two types: first, of surfaces simply indented with a Vickers pyramid at prescribed loads in air for a fixed contact period $\approx 10$ sec; second, of sections through similar indentations, obtained by positioning the Vickers pyramid at points along a pre-existing hairline crack, Fig. 6 [11–15]. Examples of the former type are shown in Figs. 7 and 8, and of the latter in Fig. 9.

Many of the important features of the indentation patterns revealed by the micrographs have been discussed at length elsewhere [14]; we simply summarize these features here, placing emphasis on those which bear on the initiation phenomenon. The radial cracks apparently initiate from within the deformation zone (as do subsurface lateral cracks [26]). Within the deformation zone well-defined displacement faults are evident by virtue of the stepped traces they leave on the specimen free surfaces; these traces, approximately parallel to the impression edges in the top view and curved below the contact centre in the side view, correspond closely to maximum shear trajectory surfaces [11]. The shear faults appear to be "ideally narrow", i.e. they do not form as slip *bands* characteristic of dislocation multiplication processes in metals. They can intersect with neighbours, generally on near-orthogonal trajectories, sometimes producing kinks in the subsurface traces, indicating some degree of continuity across the fault inter-

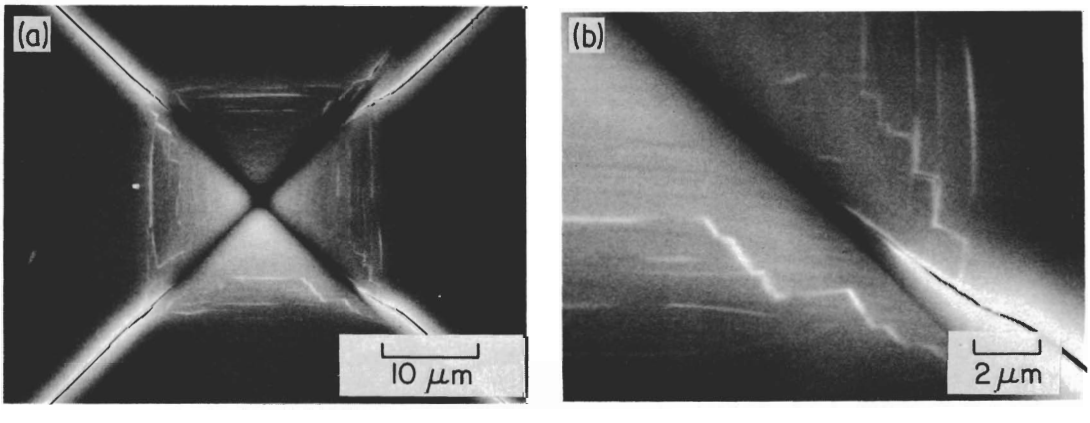


*Figure 7* Scanning electron micrograph of Vickers indentation in soda-lime glass. Surface view. Indentation load $P_m$ = 4.0 N. Micrograph (b) is an enlarged detail of right lower impression corner region in (a).

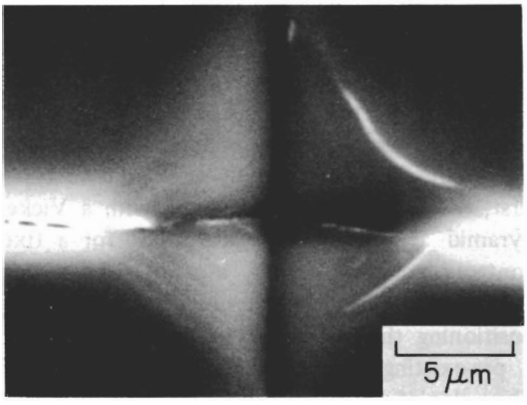


*Figure 8* Scanning electron micrograph of Vickers indentation across pre-existing crack in soda-lime glass. Surface view. Indentation load $P_m = 1.0$ N. Note apparent "welding" of pre-crack interface within compressive deformation zone.

face. These intersections can give rise to local stress intensifications, as evidenced by the formation of cavities there at higher contact loads [14].

## 3.2. Key features of the indentation patterns

The features we would emphasize as pertinent to the initiation process are as follows:

(i) The normal stresses which act across the shear faults are predominantly compressive. Evidence for this is seen in Figs. 7 and 8. In both these micrographs the radial cracks have wide residual openings outside the deformation zone but close up tightly within the inner regions of the zone. Fig. 8 is particularly interesting in this regard, for the contact appears to have "welded" together opposite faces of the pre-existing fissure. This evidence reinforces the notion of structural "continuity" across the faults and suggests, moreover, that the compressive stresses must induce significant interfacial cohesion.

(ii) Notwithstanding this predominance of compression within the deformation zone the faults appear to open up slightly, notably at the top surface where some biaxial "stretching" of the upper layers must have occurred to accommodate the increased area of the impression. Such surface openings are enhanced in the sectioned specimens, Fig. 9 (cf. Fig. 7), indicative of surface relaxation effects associated with the sectioning process itself. Thus the shear faults remain planes of weakness in the material, so the cohesion referred to in (i) above must be somewhat less than that representative of the bulk strength.

(iii) The major faults appear to be separated by a characteristic spacing, in this case of order 1 μm, but this spacing is subject to considerable variability. Accordingly, no two indentations, even when produced under ostensibly identical test conditions, produce precisely the same fault pattern; indeed, as is apparent from Fig. 7a the pattern can differ significantly in adjacent quadrants of the same impression.

(iv) The faults are constrained in their sideways expansion on the surface at the indentation diagonals (where the direction of shear strain must change abruptly to accommodate the pyramidal geometry of the indenter) and, to a lesser extent, in their downward extension by mutual intersections (interpenetration becoming increasingly difficult as kinks form [14]). Hence the scale of the critical fault is effectively determined by

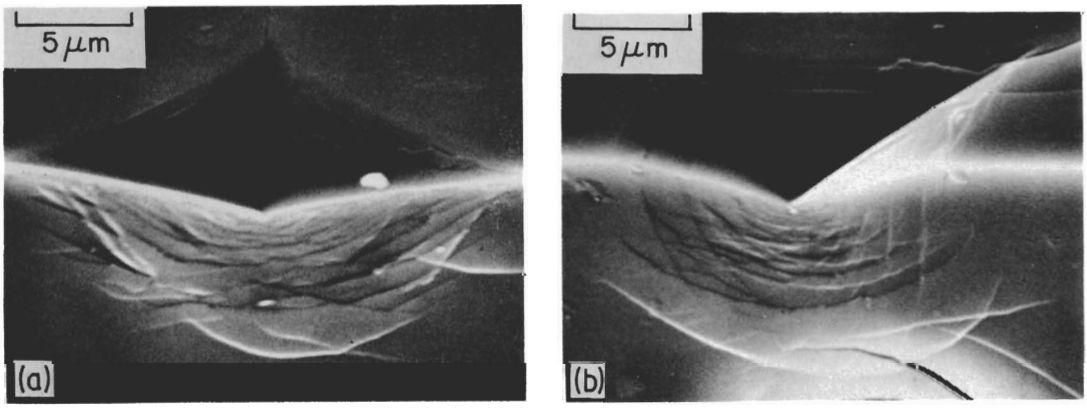


*Figure 9* Scanning electron micrograph of Vickers indentation in soda-lime glass. Surface plus section view: (a) 90° orientation, (b) 45° orientation. Indentation load $P_m = 2.0$ N.

that of the hardness impression (notwithstanding the variability factor discussed in (iii) above).

(v) The radial cracks appear to generate from the shear faults, but, because such cracks inevitably expand toward the centre of the indentation (even if only slightly, due to the high compressive stresses within the deformation zone) as well as away from it, the origins themselves are difficult to locate. In many cases there is evidence of more than one initiation attempt at any indentation corner; in the detail surface view of Fig. 7b, for instance, small crack segments approximately parallel to the impression diagonal are seen to run from near the ends of some of the inner faults, only to be arrested at the (weak) interfaces of surrounding neighbours. Thus initiation would seem to originate at or close to the surface extremity of an outer fault where the constraint is high and the potential for obstruction by neighbours is low. This conclusion suggests a certain independence of nucleation centres in adjacent quadrants, consistent with the fact that radial cracks can occasionally be made to pop-in on *both* sides of an indentation corner, as in the upper right of Fig. 7a (although the relaxation effect of the first pop-in will more often than not be sufficient to suppress its potential competitor), and with the earlier observation (Section 2.1) that the four arms of the radial pattern do not usually form simultaneously.

(vi) As the peak indentation load diminishes into the sub-threshold region the scale of the contact reduces to a level comparable with the characteristic fault spacing. Yet the surface impression remains well formed and smooth [27], suggesting that the faulting mechanism probably continues to operate continually between major slip events, albeit at a much reduced level of severity.

## 4. Crack initiation model

In this section we seek to establish a qualitative model for the radial pop-in process, consistent with the preceding experimental observations. In particular, we concern ourselves with an explanation of the incubation time, along with its dependence on moisture, stress state, etc. The model is developed in two parts, shear-activated faulting followed by tension-activated crack pop-in.

### 4.1. Formation of shear faults

The contact of a sharp-pointed indenter on a material surface produces a highly concentrated stress field. In the absence of nonlinear, irreversible deformation processes this field would be singular at the contact point. In characteristically "plastic" materials (e.g. most metals) stress relief occurs readily by the operation of dislocation multiplicative processes (or by some alternative plasticity process, such as twinning). Such dislocations usually generate at low friction levels and penetrate deep into the material, thereby accommodating the large downward displacements at the contact surface over relatively expansive slip distances. In "brittle" materials, however, low-stress regenerative processes of this kind do not operate at ordinary temperatures, and relatively high stress levels, approaching the limits of intrinsic cohesive strength, are needed to drive stress-relieving processes. In this latter case the deformation is more catastrophic in nature across the fault plane, although it is still driven predominantly by the shear component of the contact field. A distinguishing feature of such high-stress modes is the strong localization of the deformation zone about the surface impression, intensified by the geometrical constraints referred to in Section 3.2. Shear strain levels are accordingly severe in this class of materials and the tendency to elastic recovery in the impression depth is strong [28].

The slip process envisaged here for soda-lime glass is one of high-stress, intermittent shear failure along well-defined fault surfaces. As the indenter penetrates, faults are "punched" into the underlying material in the manner of Fig. 10. Minor slippage probably occurs on a much finer scale than the spacing of traces observed in the SEM observations; we have already alluded to this in our previous mention of the smooth surface impression at sub-threshold loading (Section 3.2), and there is some more direct supportive evidence from high resolution observations of closely-spaced ($\ll 1\,\mu$m), shallow, penny-like "shear defects" at low-load Knoop indentations in diamond using transmission electron microscopy (TEM) [29]. These surface-localized shear defects cannot in themselves accommodate the build-up of surface displacement at the contact interface so, at some catastrophic point, a major fault develops into the material. Some stress release must accompany the development of any such fault, which subsequently becomes encompassed within the expanding deformation zone. The stress

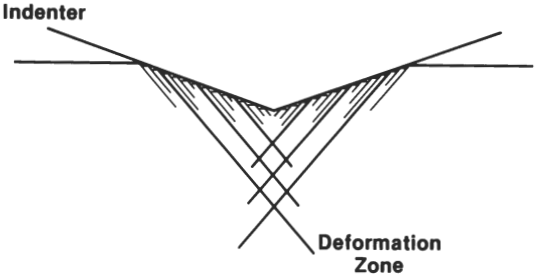


*Figure 10* Model of fault formation beneath Vickers pyramid, showing how shear displacements accommodate the pentrating indenter. Minor slip is shown occurring between major faults.

level is then able to build up again, thereby allowing the process to repeat itself.

It was agreed in Section 3.2 that compressive stresses within the deformation zone must induce some cohesion across the fault interfaces. In this context we may note that Wiederhorn and Townsend [30] showed that tensile crack interfaces in soda-lime glass can heal *spontaneously*, with strength recoveries $\approx 80\%$ in shock loading and $\approx 20\%$ in static loading, the difference in the two cases reflecting the fact that the entry of atmospheric water molecules and the ensuing saturation of primary bonds are rate limited. We might expect a shear fault which developed catastrophically and which sustains intense closure tractions in the way envisaged above to rebond at least as strongly as rapidly loaded tensile cracks. However, the degree of healing will depend on other factors as well, not least the topography of the interfacial walls [31]; for walls in sliding contact this topography is likely to be far from smooth on the molecular scale. Hence the newly formed deformation faults represent planes of substantially recovered structural integrity, yet, at the same time, of potential weakness in the glass.

Taking the analogy with tensile cracks one step further, it can be argued that any entry of water into the shear fault interfaces should cause substantial decohesion, replacing silanol bridging bonds by weak hydrogen bonds. As far as environmental access is concerned it is well known from the literature on grain boundaries in crystalline materials that high energy defect planes can provide rapid diffusion pathways [32]. The kinetics of this precursor stage in the overall crack initiation process then arise from the rate dependencies of the sequential diffusion and interaction processes. It is interesting to note that Kranich and Scholze [33] arrived at a similar conclusion in their interpretation of the observed time dependence of hardness in glass [22, 24]; their discussion centred on a water-induced "softening" effect, in which hydrolytic weakening acts to suppress recovery of indentation diagonals during unloading. Two important characteristic features may thus be associated with our fault model: first, since external water must diffuse into the interfaces via the top surface (where, it will be recalled, there is a tendency to a slight opening), the decohesion depth will be limited, especially at the faster contact rates; second, since it is the shear component of the stress field which creates the fault in the first place, the decohesion of the restored interfacial bonds is presumably also shear-activated.

## 4.2. Initiation of radial cracks

The initiation of a radial crack occurs when a favourably disposed shear fault within the contact field reaches a critical stress intensification. There would appear to be two distinctive ways in which this intensification might be achieved. The first is by classical subcritical growth of a microcrack [34]. In this interpretation it is acknowledged that the microcrack can originate from the edge of a shear fault; however, the kinetics of the pop-in event are essentially due to moisture-enhanced "slow" growth in some tensile region of the field (although this growth could conceivably, at least at its inception, involve some "mixed mode", i.e. combined shear plus tension). The second is by interfacial debonding of the shear faults themselves, as discussed in Section 4.1. Again, it is taken that fracture will originate from the faults, but this time the fault edges are constrained; it is now the shear-activated decohesion process which is rate controlling. The distinction here is not trivial, for the basic rate equations could conceivably have entirely different forms in the two cases, and it is such basic equations which must ultimately provide the starting point for any proper theory of fatigue in the sub-threshold region.

At this point it is useful to recall the major features of the kinetic observations that our crack initiation model will need to explain. First, it is necessary to account for the roles of the two test variables, water concentration and indentation load, on the incubation time. Then we

should be able to show why at long contact periods the pop-in time is reproducible and insensitive to the test variables and, conversely, why at short contact periods it is not. Again, our model should indicate why the rate of radial crack development *after* indentation is lower than that *during* indentation at any given load, and why this rate tends to diminish further as the contact period is decreased.

Consider these points in relation to Fig. 11. This schematic representation, drawn from the SEM observations, shows a fault FF developing from one of its ends into a radial crack FC. The fault is driven by the shear stress SS and the crack by the normal stress NN. A complete evaluation of these two stress terms over the respective planes at any given stage of the indentation cycle is a complex task requiring, among other things, explicit knowledge of the constitutive laws for the deformed material and facility for incorporating details of the contact geometry [8]. Nevertheless, by recognizing that the general indentation field may be subdivided into reversible and irreversible components [9], simplistic elastic/plastic analyses may be used to determine some of the broader features [10]. Accordingly, Fig. 12 indicates how the level of the two pertinent stress terms at the contact surface may vary through the cycle. The shear SS, which must be determined largely by the indenter angle (Fig. 10), reaches a maximum value at full loading; on removing the indenter elastic recovery occurs in the penetration depth [28], effectively reducing the contact angle, thereby leaving a residual stress of diminished magnitude but of same sign acting on the fault. The normal stress NN has a slightly more subtle evolution, owing to the fact that the reversible and irreversible components oppose each other [10]: at full loading the elastic component dominates, and because this term is compressive in the surface region* the net stress is also compressive; on unloading the indenter only the inelastic component remains, and so the normal residual stress is tensile. Thus there is a "cross-over point" in the unloading where the driving force on the radial crack plane abruptly becomes positive; this feature is consistent with the observation (Section 2.2) that well-developed radial cracks tend to close up at their surface on reloading the indenter beyond the preceding critical unload point (in our case at $P_c = 0.3\,P_m$).

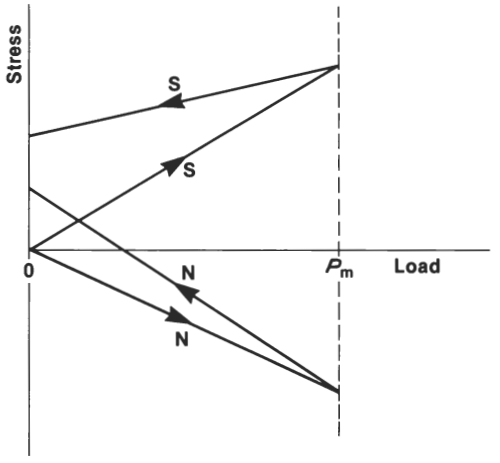


*Figure 12* Intensity variation of shear SS and normal NN stresses (Fig. 11) through indentation cycle. Whereas during the unloading half-cycle SS simply reduces in magnitude to residual level, NN actually reverses sign, at $P \simeq 0.3\,P_m$, en route to its ultimate tensile state.

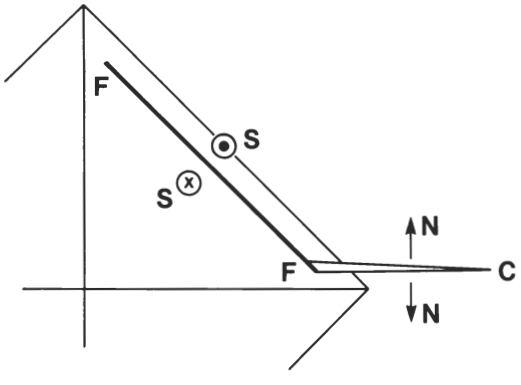


*Figure 11* Model of radial crack initiation FC from fault FF, in one quadrant of Vickers impression. Shear SS and normal NN stresses provide driving forces for fault and crack, respectively.

The question now is, are the kinetics controlled by a subcritical stage of the crack growth along FC or by fault decohesion at FF in Fig. 11? Let us attempt to analyse the experimental evidence in terms of these two possibilities.

### 4.2.1. Test variables; role of water and contact load

We have already indicated that both crack growth [17, 19] and fault decohesion [33] (Section 4.1) are sensitive to water in the external environment.

*In the subsurface region beneath the indenter this same component is tensile, the implications of which we shall pursue in the Section 5.

In each case there is a two-step process, diffusion followed by interaction, the rates of which increase in some simple proportion with chemical activity. On the face of it, therefore, both potential models would appear to account for the curve shifts in Fig. 5 to shorter times with increasing moisture content.

A similar conclusion may be drawn concerning the contact load. The main effect of increasing $P_m$ is to increase the fault *size,* without changing the intensity or geometrical distribution of stresses over the fault surface (similitude principle) [2, 10]. The stress intensification in turn is expected to increase with fault size, but only modestly (fractional power) [34], for any given diffusion or interaction conditions. This is again consistent with the slow data trends to shorter times at higher loads in Fig. 4.

Hence as far as the basic chemical and stress effects are concerned there is little to distinguish between the two candidate models in accounting for *qualitative* variations in incubation times.

### 4.2.2. Effect of contact period on incubation time

For contact periods $T$ greater than the pop-in time $t_c$ the critical nucleus, whatever its nature, has developed beyond the configuration at which unstable fracture must occur spontaneoulsy in tensile loading. It is evident from Fig. 12 that such spontaneous fracture cannot occur at peak loading, for there the pertinent normal stresses are compressive; the indenter has to be unloaded to $\simeq 0.3\ P_m$ before tensile driving forces may be realized. In this time region, therefore, the pop-in event is determined predominantly by the stress field characteristics (more specifically, by its constraint characteristics), so the kinetics of the nucleation event itself are not manifest in the data, provided there is always a sufficient density of faults to guarantee a suitable nucleation centre.

At $T \ll t_c$ the development of a critical nucleus is clearly completed *after* the indentation cycle. It is now the residual components of stress which drive the initiation. As seen from Fig. 12 a positive driving force for fracture exists throughout the post-indentation period, so pop-in occurs immediately the precursor nucleus becomes critical. In this domain, therefore, the kinetics of the nucleation event itself and the variables which control this event are reflected directly in the data. Any factors which militate against exact reproducibility of events from indentation to indentation will likewise reflect in the data scatter. In this regard the variability of the fault patterns noted in the SEM observations (Section 3.2) is pertinent, particularly in mind of the notoriously high gradients of stresses (from which the overall crack driving force must ultimately be determined) which characterize the near fields in general contact problems [8].

Again, it is not clear that any qualitative distinction can be made between models in explaining the transition from in-cycle to post-cycle crack initiation as the contact period diminishes; any rate-limiting process consistent with the dependence on water content and contact load as discussed in Section 4.2.1 above would seem to be capable of acounting for incubation phenomena of this kind.

### 4.2.3. Pop-in rate; effect of different stress component, contact period and temperature

We may note from Fig. 3 that, for given environmental and loading conditions, there is an intermediate range of contact periods within which initiation occurs with comparable frequencies during and after the contact. In the latter case, however, the pop-in time is relatively long, i.e. $t_c \gg T$. This implies that the development of a critical nucleus continues after indenter removal, but at a reduced rate relative to that at full load. Reference once more to Fig. 12 indicates that the stress component responsible for providing the initiation driving force must be the shear SS rather than the tension NN, for the latter increases on unloading. Unfortunately, this still does not help us in distinguishing between the models, for both the growth of a microcrack from the fault edge and the decohesion of the fault itself would tend generally to diminish in velocity upon reducing the shear intensification. Of course, the microcrack mechanism would tend also to rise in velocity under the simultaneous action of the increasing tensile loading; whether this tensile component of driving force should be sufficient to dominate the shear contribution, in which case the microcrack hypothesis would no longer comply with experimental observation, can only be answered by a quantitative analysis.

We further recall from Fig. 3 that the time to pop-in tends to increase as the contact period is systematically reduced below the incubation

period. This observation is consistent with the argument presented in the preceding paragraph; reducing $T$ is equivalent to reducing the time interval in which the nucleus grows at its fastest velocity.

The fact that immersion of air-indented specimens into hot water rapidly accelerates the pop-in rate (Section 2.2) serves to indicate that the appropriate rate-controlling process is thermally activated, as expected for general interfacial diffusion and reaction processes.

## 5. Discussion

We have presented evidence for strong kinetic effects in the threshold for radial fracture. In particular, we have shown that there exists an incubation time for crack pop-in, and that this time is reduced as the moisture content or peak contact load is increased. We have also presented SEM micrographs which demonstrate the role of shear faults in the precursor initiation process. Two possible models have been considered in our attempts to account for the observations, one based on the notion of microcrack expansion from the edge of a critical fault and the other on the progressive decohesion of the fault interface itself. Both models involve a two-step, diffusion-interaction sequence. Our qualitative interpretations of the data have not allowed us to distinguish between the two models, although it has been established that the vital component of the stress field in driving the initiation is the shear across the precursor fault and not the tension across the ultimate crack.

These results, despite their lack of conclusiveness, are useful in the way they highlight the rapidly changing nature of strength-controlling flaws in the sub-threshold region. The emphasis shifts from classical crack extension to deformation fault energetics. On entering the realm of ultra-small scale flaws, therefore, one may need to adopt an entirely new physical base for analysing such flaw-related properties as strength, wear and erosion, grinding and polishing, etc [3]. For this reason alone it would appear reasonable to advocate more quantitative treatments of the two models discussed above, along with a broader experimental investigation into extraneous variables, in an attempt to obtain definitive answers. Studies of other materials, including "anomalous" glasses [12], which tend to deform by densification rather than by slip processes, and crystalline materials, which tend to slip on restricted crystallographic planes, could prove valuable, if only to establish the generality of the phenomenon.

Of the flaw-related properties mentioned above, strength is perhaps the one which has been studied most systematically in relation to the sub-threshold transition [4, 16]. The most distinctive feature on undergoing this transition from the domain of well-developed cracks is an abrupt increase in the strength level, demonstrating that the sub-threshold flaw is not nearly as potent as its post-threshold counterpart as a source of degradation. Nevertheless, the former flaw type does still provide preferred sites for failure in glass surfaces of otherwise pristine condition (e.g. optical fibres), emphasizing the significantly weakened structure of the shear fault interface. The mode of failure envisaged here is one of augmentation of the residual shear stress on the fault by the applied tensile loading, Fig. 13. This augmentation may occur in either of two ways: directly, by enhancing the shear stress itself; or indirectly, by negating the compressive stress. The abrupt strength increase referred to above arises because one now has to initiate the radial crack before any propagation instability can be attained, and to effect initiation the applied loading has first to compensate for the relaxation of shear driving force that occurs during the preceding contact evolution. The fact that the spontaneous pop-in rate is severely retarded in tempered glass (Section 2.2) is in line with this description; the surface compression acts in the opposite direction, diminishing the stress intensification rather than enhancing it.

There are two other distinguishing features

*Figure 13* Schematic showing augmentation of residual stress configuration at indentation fault by applied tensile field. The tensile load may be resolved into components at the fault plane which reinforce the residual shear and negate the residual compression.

of the strength properties for sub-threshold flaws which bear comment here [16]. The first is the relatively large scatter in results obtained under ostensibly invariant indentation test conditions. Such scatter is consistent with that observed in the delayed pop-in data in Fig. 3, associated with the variability in the fault patterns as noted in the SEM studies. What causes this variability in the first place is a question that we cannot answer without a deeper understanding of the fault micromechanics, including, presumably, information on the nature and distribution of the underlying slip nucleation centres. The second of the additional features which accompanies the sub-threshold transition is the enhanced susceptibility to "fatigue", as reflected in a steeper slope in standard logarithmic strength against stress rate plots. An increased susceptibility of this kind could be due to a change in failure mechanism, i.e. fault decohesion. However, it is also possible to explain the trend in terms of the microcrack hypothesis; the presence of a strong residual-contact component in the fracture driving force can lead to significant increases in "apparent" crack velocity exponents [35]. Again, quantitative modelling of the candidate processes would seem to be called for.

Throughout our presentation we have been working on the premise that the radial cracks initiate at or close to the indentation surface. The normal stresses on the crack plane become tensile at the surface only after substantial withdrawl of the indenter; in the subsurface regions, however, these same stresses are tensile at *all* stages of the contact cycle [10]. Thus at higher indentation loads we might expect the stress intensity for initiation to be exceeded during the first half-cycle, with an attendant switch from surface (radial) to subsurface (median) crack formation [10, 26]. Such behavioural changes in the geometrical aspects of indentation fracture have indeed been observed [11, 36]. The main influence of kinetic effects in this dichotomy is in the radial fracture threshold; the surface regions do of course have direct access to the environment and are accordingly more susceptible to the rate-sensitive hydrolytic weakening. In this way estimates of the lower limits to indentation-induced pop-in based strictly on equilibrium concepts [2, 34, 37] could be in serious error, on the nonconservative side in the context of strength design.

Finally, a comment may be made concerning the nature of the shear fault interfaces as envisaged in this study. The major shear displacements take place catastrophically, close to the level of cohesive strength, without dislocation regenerative processes. The resulting net configuration is nevertheless one which might be represented, mathematically at least, by a pile-up of dislocations. Is such a configuration more accurately defined as a slip surface or a shear crack? In ceramics and glasses with intrinsically strong bonding characteristics the distinction between deformation and fracture processes may not always be as clear cut as it is for materials with well-defined yield stresses.

## Acknowledgements

The authors wish to thank R. F. Cook, E. R. Fuller, B. J. Hockey, D. B. Marshall, R. S. Polvani, M. V. Swain, and R. M. Thomson for many stimulating discussions during this study. R. F. Cook also performed the delayed hot water tests referred to in Section 2.2, and R. S. Polvani set up parts of the hardness testing apparatus. Funding was provided by the US Office of Naval Research, Metallurgy and Ceramics Program.

## References

1. B. R. LAWN and T. R. WILSHAW, "Fracture of Brittle Solids" (Cambridge University Press, London, 1975) Chaps. 1 and 2.
2. B. R. LAWN and A. G. EVANS, *J. Mater. Sci.* **12** (1977) 2195.
3. B. R. LAWN and D. B. MARSHALL, *J. Amer. Ceram. Soc.* **62** (1979) 347.
4. T. P. DABBS, D. B. MARSHALL and B. R. LAWN, *ibid.* **63** (1980) 224.
5. T. P. DABBS and B. R. LAWN, *Comm. Amer. Ceram. Soc.* **65** (1982) C-37.
6. D. J. GREEN, in "Fracture Mechanics of Ceramics", edited by R. C. Bradt, A. G. Evans, D. P. H. Hasselman and F. F. Lange (Plenum Press, New York, 1982).
7. B. R. LAWN, *J. Amer. Ceram. Soc.* **66** (1983) 83.
8. B. R. LAWN and T. R. WILSHAW, *J. Mater. Sci.* **10** (1975) 1049.
9. D. B. MARSHALL and B. R. LAWN, *ibid.* **14** (1979) 2001.
10. B. R. LAWN, A. G. EVANS and D. B. MARSHALL, *J. Amer. Ceram. Soc.* **63** (1980) 574.
11. J. T. HAGAN and M. V. SWAIN, *J. Phys. D: Appl. Phys.* **11** (1978) 2091.
12. A. ARORA, D. B. MARSHALL, B. R. LAWN and M. V. SWAIN, *J. Non-Cryst. Solids* **31** (1979) 415.
13. J. T. HAGAN, *J. Mater. Sci.* **14** (1979) 462.
14. *Idem, ibid.* **15** (1980) 1417.
15. K. PETER, *J. Non-Cryst. Solids* **5** (1970) 103.

16. T. P. DABBS and B. R. LAWN, *Phys. Chem. Glasses* **23** (1982) 93.
17. S. M. WIEDERHORN, *J. Amer. Ceram. Soc.* **50** (1967) 407.
18. S. M. WIEDERHORN and L. H. BOLZ, *ibid.* **53** (1970) 543.
19. D. T. GRIGGS and J. D. BLACIC, *Science* **147** (1965) 292.
20. D. T. GRIGGS, *Geophys. J. R. Astr. Soc.* **14** (1967) 19.
21. C. H. SCHOLZ and R. J. MARTIN, *J. Amer. Ceram. Soc.* **54** (1971) 474.
22. S. P. GUNASEKERA and D. G. HOLLOWAY, *Phys. Chem. Glasses* **14** (1973) 45.
23. V. R. HOWES, *Glass Tech.* **15** (1974) 148.
24. C. J. FAIRBANKS, R. S. POLVANI, S. M. WIEDERHORN, B. J. HOCKEY and B. R. LAWN, *J. Mater. Sci. Lett.* **1** (1982) 391.
25. M. WADA, H. FURUKAWA and K. FUJITA, in Proceedings of the 10th International Congress on Glass, Vol 11, (Ceramic Society of Japan, Tokyo, 1974) p. 39.
26. B. R. LAWN and M. V. SWAIN, *J. Mater. Sci.* **10** (1975) 113.
27. T. P. DABBS and B. R. LAWN, to be published.
28. B. R. LAWN and V. R. HOWES, *J. Mater. Sci.* **16** (1981) 2745.
29. P. HUMBLE and R. H. J. HANNINK, *Nature* **273** (1978) 37.
30. S. M. WIEDERHORN and P. R. TOWNSEND, *J. Amer. Ceram. Soc.* **53** (1970) 486.
31. B. J. HOCKEY and B. R. LAWN, *J. Mater. Sci.* **10** (1975) 1275.
32. P. G. SHEWMON, "Diffusion in Solids" (McGraw-Hill, New York, 1963) Chap. 6.
33. J. F. KRANICH and H. SCHOLZE, *Glastechn. Ber.* **49** (1976) 135.
34. S. S. CHIANG, D. B. MARSHALL and A. G. EVANS, *J. Appl. Phys.* **53** (1982) 312.
35. E. R. FULLER, B. R. LAWN and R. F. COOK, *J. Amer. Ceram. Soc.* in press.
36. H. ISHIKAWA and N. SHINKAI, *Comm. Amer. Ceram. Soc.* **65** (1982) C-124.
37. J. T. HAGAN, *J. Mater. Sci.* **14** (1979) 2975.

*Received 7 February*
*and accepted 15 February 1983*